Global Iron Connections Between Desert Dust, Ocean Biogeochemistry, and Climate

T. D. Jickells,[1] Z. S. An,[2] K. K. Andersen,[3] A. R. Baker,[1] G. Bergametti,[4] N. Brooks,[1] J. J. Cao,[2] P. W. Boyd,[5] R. A. Duce,[7] K. A. Hunter,[6] H. Kawahata,[8] N. Kubilay,[9] J. laRoche,[10] P. S. Liss,[1] N. Mahowald,[11] J. M. Prospero,[12] A. J. Ridgwell,[13] I. Tegen,[14]* R. Torres[15]

The environmental conditions of Earth, including the climate, are determined by physical, chemical, biological, and human interactions that transform and transport materials and energy. This is the "Earth system": a highly complex entity characterized by multiple nonlinear responses and thresholds, with linkages between disparate components. One important part of this system is the iron cycle, in which iron-containing soil dust is transported from land through the atmosphere to the oceans, affecting ocean biogeochemistry and hence having feedback effects on climate and dust production. Here we review the key components of this cycle, identifying critical uncertainties and priorities for future research.

Iron is an essential nutrient for all organisms, used in a variety of enzyme systems, including those for photosynthesis, respiration, and nitrogen fixation (1, 2). However, iron is very insoluble under oxidizing conditions above pH 4 (3). For marine phytoplankton, separated from the iron-rich sediment of the ocean floor by considerable water depths,

[1]School of Environmental Sciences, University of East Anglia, Norwich NR47TJ, UK. [2]State Key Lab of Loess and Quaternary Geology, Institute of Earth Environment, Chinese Academy of Sciences, AS, 10 Fenghui South Road, Post Office Box 17, China. [3]Niels Bohr Institute, University of Copenhagen, Juliane Maries Vej 30, 2100 Copenhagen, Denmark. [4]Laboratoire Interuniversitaire des Systèmes Atmospherique, Universités Paris 7 and Paris 12, UMR CNRS 7583, Paris, France. [5]National Institute of Water and Atmospheric Research Centre for Chemical and Physical Oceanography, Department of Chemistry; [6]Department of Chemistry, Post Office Box 56; University of Otago, Dunedin, New Zealand. [7]Departments of Oceanography and Atmospheric Sciences, Texas A&M University, TAMU 3146, College Station, TX 77843–3146, USA. [8]Geological Survey of Japan, National Institute of Advanced Industrial Science and Technology (AIST), Tsukubahigashi 1-1-1, Ibaraki 305–8567, Japan. [9]Institute of Marine Sciences, Middle East Technical University, Post Office Box 28, Erdemli-Mersin 33731, Turkey. [10]Leibniz-Institute für Meereswissenschaften IFM-GEOMAR, Marine Biogeochemistry, Gebäude Westufer, Düsternbrooker Weg 20, 24105 Kiel, Germany. [11]National Center for Atmospheric Research. Post Office Box 3000, Boulder, CO 80307, USA. [12]Rosenstiel School of Marine and Atmospheric Sciences, University of Miami, 4600 Rickenbacker Causeway, Miami, FL 33149–1089, USA. [13]Department of Earth and Ocean Sciences, University of British Columbia, 6339 Stores Road, Vancouver, British Columbia V6T 1Z4 Canada. [14]Max-Planck-Institute for Biogeochemistry. Post Office Box 10, 01 64 07701 Jena, Germany. [15]Universidad de Conception, Departamento de Oceanografia, Casilla 160C, Chile.

*Present address: Institute for Tropospheric Research, Permoserstrasse 15 04318, Leipzig, Germany.

physiological iron requirements must be met from within the water column. Iron supply is a limiting factor on phytoplankton growth over vast areas of the modern ocean, although this may not have been so in the distant past, when prokaryotes first evolved in a less oxic ocean (1).

Iron supply reaches the oceans mainly from rivers as suspended sediment in a vast global transport system (Table 1). However, fluvial and glacial particulate iron is efficiently trapped in near-coastal areas (4), except where rivers discharge directly beyond the shelf. Hydrothermal inputs are rapidly precipitated at depth in the oceans. Hence, the dominant external input of iron to the surface of the open ocean is aeolian dust transport, mainly from the great deserts of the world. Currently hyper-arid areas such as the Sahara desert occupy 0.9 billion hectares and drylands occupy 5.2 billion hectares, which is one-third of global land area. These environments are particularly sensitive to global change pressures (5, 6), and such changes could alter ocean productivity and hence climate. There are other possible contributors to atmospheric iron supply, including volcanic, anthropogenic, and extraterrestrial sources (7, 8), whose iron may be more soluble than iron in soil aluminosilicates (7), and these merit further study.

Dust produced in arid areas has important and disparate effects throughout the Earth system, as illustrated in Fig. 1 and discussed below. These need to be incorporated into climate models to correctly predict impacts of global change pressures. We first consider each component of the system before attempting a global synthesis.

Climate Effects on Dust/Iron Fluxes

Satellite imagery has greatly increased our knowledge of large-scale dust source regions, emphasizing the importance of localized sources, which vary seasonally. There are similar climatic and geomorphological controls on many source regions (6), and dried-out lake systems such as the Bodele Depression in North Africa appear to be particularly important. Dust production depends on the supply of wind-erodible material, which ironically usually requires fluvial erosion, often from adjacent highlands, followed by subsequent drying out and the loss or absence of vegetative protection (6, 9–11). Dust production arises from saltation or sandblasting, when winds above a threshold velocity transport soil grains horizontally, producing smaller particles, a small proportion of which get carried up into the atmosphere for long-range transport. These processes depend on rainfall, wind, surface roughness, temperature, topography, and vegetation cover, which are interdependent factors linked to aridity and climate in a highly nonlinear way. Wind tunnel studies show dust production to be proportional to the cube of wind speed (5).

Desert dust aerosol is dominated by particles of diameter 0.1 to 10 μm, with the mean size being around 2 μm. Such aerosols have a lifetime of hours to weeks, allowing long-range transport over scales of thousands of

Table 1. Global iron fluxes to the ocean (in Tg of Fe year^{-1}). From Poulton and Raiswell (4), with modified atmospheric inputs from Fig. 2. "Authigenic fluxes" refer to releases from deep-sea sediments during diagenesis. We distinguish only separately dissolved and particulate for fluvial inputs, because it is clear that fluvial particulate iron, along with iron from coastal erosion and glacial sediment sources, does not reach the oceans, whereas authigenic, atmospheric, and hydrothermal iron all reach the oceans regardless of their phase.

Source	Flux
Fluvial particulate total iron	625 to 962
Fluvial dissolved iron	1.5
Glacial sediments	34 to 211
Atmospheric	16
Coastal erosion	8
Hydrothermal	14
Authigenic	5

kilometers (*5*, *11*) but producing strong gradients of dust deposition and concentrations that vary substantially on time scales of ~1 day. Dust production, transport, and deposition to the oceans again depend on climatic factors, particularly atmospheric structure, which regulates uplift, and wind speed and precipitation, which influence removal. Much of the transport of dust occurs at altitudes of several kilometers, with subsequent removal by wet deposition. Hence, satellite images of dust may not reflect dust inputs to the oceans (*7*).

Dust removal occurs by wet and dry deposition, processes whose efficiency varies with aerosol particle size (*7*). Measurements at a limited number of sites and modeling studies suggest that 30 to 95% of total removal is by wet deposition (*7*, *12*). Wet deposition is spatially variable, reflecting several climatically sensitive factors, including aerosol size distribution, rainfall patterns, and transport altitude. This results in considerable uncertainties in estimating the contribution of wet deposition to total deposition.

Dust fluxes can be estimated from direct measurements and subsequent extrapolation (*13*), models (*11*, *14*, *15*), and satellite observations (*16*). The various approaches all yield similar dust deposition estimates of 1000 to 2000 Tg year^{-1} (1 Tg = 10^{12}g), varying substantially from year to year. However, models are usually tuned to match observations, and hence the agreement is not truly an independent validation.

Existing models of global dust transport (*14*, *15*) include only first-order physical representations of the key dust production processes, largely because of the lack of suitable data sets of global surface characteristics. Despite this, global models seem able to simulate dust deposition fluxes reasonably well. We estimate production at 1700 Tg year^{-1}, with almost two-thirds from North Africa and 26% of the dust reaching the oceans (Fig. 2). Changes in the hydrological cycle and/or vegetative cover affect global dust production (*10*) as recorded over glacial/interglacial cycles in loess, ice core, and marine sediment records. Dust fluxes were 2 to 20 times higher during the last glaciation (*17*–*19*) because of stronger winds, aridity, changes in vegetation cover, lowered sea level, and reduced precipitation. It has been suggested that changing land use practices over recent decades have altered dust fluxes by up to 50% (*14*, *20*), although recent work suggests lower values (*15*). Although the global importance of land use change as a dust source is currently uncertain, effects at a regional scale are clear, such as around the Aral Sea and the in the U.S. 1930s Dust Bowl storms (*6*). Dust storm frequency over the Sahel appears to have increased since 1950. This may be related to multidecadal-scale climate variability or land use change (*21*). Dust transport over China, the United States, and North Africa has been related to large-scale climatic cycles (*22*–*26*), and the variability in dust transport can be influenced by climatic cycles such as El Niño–Southern Oscillation and North Atlantic Oscillation (*23*, *24*). Some climate models suggest that enhanced greenhouse warming could "green" the Sahel and southern Sahara (*14*, *27*), drastically altering global dust production. Different models of global dust flux
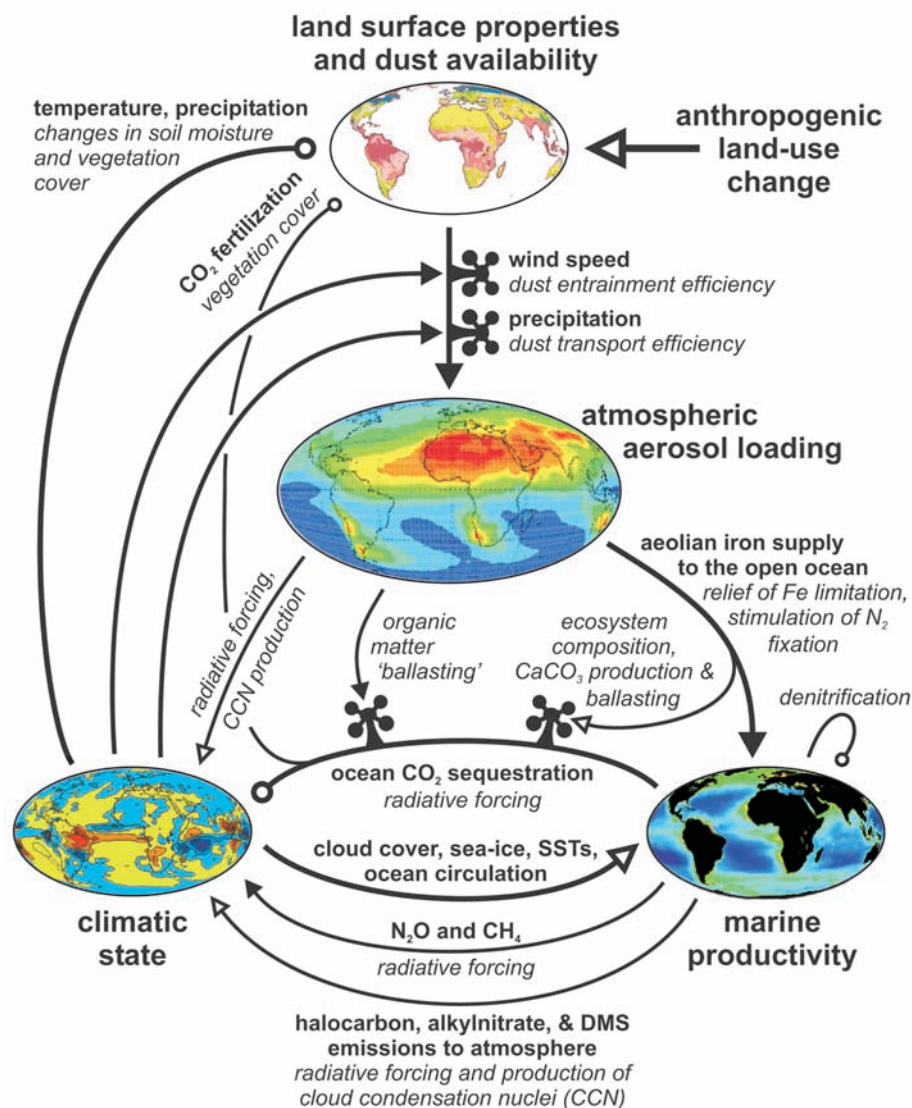

Fig. 1. Schematic view of global iron and dust connections. Highlighted are the four critical components (clockwise from top): the state of the land surface and dust availability, atmospheric aerosol loading, marine productivity, and some measure of climatic state (such as mean global surface temperature). The sign of the connections linking these varies; where the correlation is positive (for example, increased atmospheric aerosol loading → increased marine productivity), the line is terminated with a solid arrowhead. Where the correlation is negative (for example, increased marine productivity → lower CO₂ and a colder climate), the termination is an open circle. Connections with an uncertain sign are terminated with an open arrowhead. The mechanism by which the link acts (for example, the impact of a change in atmospheric CO₂ is via the radiative forcing of climate) is displayed in italics. Finally, the "water tap" symbols represent a secondary mechanism modulating the effect of a primary mechanism; for instance, a change in global precipitation strength and distribution will alter the efficiency with which entrained dust is transported to the open ocean. If a path of successive connections can be traced from any given component back to itself, a closed or feedback loop is formed. An even number (including zero) of negatively correlated connections counted around the loop gives a positive feedback, which will act to amplify a perturbation and tend to destabilize the system. Conversely, an odd number of negative correlations gives a negative feedback, dampening any perturbation and thus stabilizing the system. For instance, atmospheric aerosol loading → marine productivity → climatic state → dust availability → atmospheric aerosol loading contains two negative and two positive correlations and thus is positive overall. In contrast, marine productivity looping back onto itself contains a single negative correlation and thus represents a negative feedback.

Table 2. Effects of dust/iron (Fe) on ocean biogeochemistry. (In addition, there are dust effects on the climate system via albedo and the hydrological cycle; see text.)

Interaction	Mechanism	Area*	Reference
Primary productivity	Reduction in Fe limitation allows more efficient use of macro-nutrients and hence CO_2 uptake.	HNLC and other Fe-limited areas	(36, 42)
N_2 fixation	Reduction in Fe limitation on nitrogen fixation increases primary production and hence CO_2 uptake.	Subtropical gyres	(1, 43)
Changes in species composition	Species-selective relief of iron stress.	Global	(42)
Ballast effect	Increases sinking rate of organic matter, reducing organic matter regeneration within seasonal mixed layer; promotes CO_2 uptake.	Probably only significant in areas of high dust deposition	(52)
DMS	Increased productivity leads to increased DMS emissions and increased aerosol formation.	HNLC and other Fe-limited areas	(54)
N_2O and NO_3^-	Increased fluxes of organic matter to deep waters lower oxygen concentrations and promote denitrification, release N_2O, and lower oceanic nitrate inventory.	Upwelling systems	(53)
N_2O and CH_4	Increased productivity leads to changes in euphotic zone methane and N_2O concentrations.	HNLC and other Fe-limited areas	(54, 57)
H_2S	Increased fluxes of organic matter to deep waters lower oxygen concentrations and promote sulfate reduction; sulphide production lowers iron inventory.	Upwelling systems	
Halocarbons and alkyl nitrates	Biogenic gases linked to primary productivity. These are greenhouse gases, linked to aerosol formation and to the ozone cycle.	As for DMS	(54)
Isoprene and CO	Biogenic trace gases linked to primary productivity. These gases influence atmospheric oxidizing capacity.	As for DMS	(54, 57)

*Most impacts have effects throughout the oceans, but where appropriate, we identify here areas that are most sensitive to changes in dust/iron flux.

(14, 15) predict similar present-day dust fluxes (Fig. 2), but their predictions for the next 100 years range from a modest increase (+12%) to a significant decrease (–60%), with different regional deposition patterns. These differences reflect variations in the relative importance of land use changes and CO_2 fertilization, as well as differences in climate predictions.

Dust has important but uncertain direct impacts on climate and radiative budgets (20, 28) and possibly rainfall patterns (29). We note the importance of these physical effects but focus here on the biogeochemical effects. In a biogeochemical context, the key flux to the oceans is not dust, but soluble or bioavailable iron. Although the iron content of soil dust (average, 3.5%) is variable globally, the uncertainty introduced with this variability is small compared with other uncertainties in the iron cycle (7). Iron solubility from soil dust is low [<1 to 2% (7)]. Higher solubilities of aerosol iron have been reported (12). The controls on aerosol iron solubility include photochemistry (photoreduction of Fe III to Fe II) and acidity, particularly during aerosol cloud processing (7). Emissions of acid precursors (SO_2 and NO_x) have more than doubled from the preanthropogenic state, and NO_x emissions are expected to continue to increase (20). Organic complexation may play a role in regulating atmospheric iron solubility. Consequently, emissions of organic matter from natural sources (such as soil humic acids and plant terpenes) and anthropogenic sources (such as biomass burning and industrial/urban emissions) may influence atmospheric iron cycling (7). We know very little about the organic chemistry of aerosols or of the active microbial community identified in aerosols, which may influence iron solubility (7, 30). All these factors (acidity, organic complexation, and photochemistry) will alter with global change pressures.

Dust/Iron Impacts on the Ocean

The physicochemical environment of atmospheric iron changes dramatically on entering the oceans. At a seawater pH of 8, soluble ferric iron rapidly reprecipitates, setting up a competition between adsorption to water column particulates, active biological uptake, and organic complexation, which evolves over the surface water residence time of dust [tens of days (31)]. Experimental measurements of the solubility of aerosol iron have generally been conducted over shorter time scales and hence may not adequately predict the solubility of aerosol iron.

Measuring total and speciated iron concentrations in the ocean is difficult, but global data are now emerging (32). Total dissolved iron shows nutrient-like oceanic profiles, with low surface water concentrations (0.03 to 1 nmol liter^{-1} where photochemically produced Fe II may be significant) increasing to deep water concentrations of 0.4 to 2 nmol liter^{-1} (32, 33). Significant colloidal iron is present in the water column and is potentially biogeochemically labile (32). The impact of atmospheric deposition on surface water iron concentrations has been demonstrated (34), as has recycling from sediments and coastal regions (35, 36). Within the oceans, dissolved iron is predominantly organically complexed, stabilizing it against rapid scavenging (37), although its residence time is still probably only decades (32, 33). The source, biological function, and

structure of these organic iron-complexing ligands are essentially unknown. Electrochemical titrations suggest that some have similar binding strength to that of true siderophores: strong iron-specific ligands (3, 33, 37). Siderophores have been found in marine bacteria and coastal seawater (38). Although many species may be able to use siderophore-bound iron, siderophore synthesis systems are not readily identifiable in the genomes of important picophytoplankton species such as *Synecochoccus* and *Prochlorococcus* (39, 40), though they may be present in *Trichodesmium* and *Crocosphaera* (two marine diazotrophs) and in uncultured heterotrophic bacterial genomes from the Sargasso Sea (41).

Iron limitation reflects deep-water Fe/N concentration ratios that are inadequate to meet phytoplankton iron requirements (36) because of scavenging of iron regenerated from sinking organic matter in the deep ocean at faster rates than N. Thus, sustaining open ocean phytoplankton primary production requires an additional input of iron to that produced from upwelling, which is usually atmospheric. The relative importance of atmospheric and upwelling sources varies throughout the oceans (36). Iron limitation of phytoplankton primary production in as much as 30% of the oceans has now been suggested (1, 36, 42). In some areas, such as the Southern Ocean, this results in incomplete use of macronutrients (N, P, and Si) and relatively low algal abundance, hence the term "high-nutrient low-chlorophyll" (HNLC) regions. Recent studies emphasize more complex interactions within the ocean than simple iron limitation or sufficiency, with evidence in some areas of simultaneous limitation of primary production by iron, light,

macronutrients (*42*, *43*), and trace nutrients (such as Co and Zn) (*2*, *44*). Furthermore atmospheric inputs supply not only iron but also other nutrients and carbonate, which may influence ocean biogeochemistry (*45*, *46*).

Luxury iron uptake has been demonstrated for some phytoplankton, allowing them to better adapt to episodic atmospheric supply (*47*). Iron availability influences algal community structure as well as overall productivity. Open ocean phytoplankton generally need less iron than coastal species, which have evolved in a more iron-rich environment, although iron-limited coastal systems are known (*36*). A reduced iron requirement can be achieved by reducing cell size or minimizing the number of iron-containing enzymes (*39*). The success of *Prochlorococus* in HNLC areas depends on both strategies. Relief of iron stress results in the growth of phytoplankton taxa characterized by larger cells, particularly diatoms with less dense opal skeletons (*36*). A similar process may arise for coccolithophores as a result of Fe/Zn co-limitation (*44*). Changes in skeleton density should influence sinking rates and hence carbon export to depth, although this has not been seen in field experiments (*48*). Changes in coccolithophore abundance directly affect atmospheric partial pressure of CO_2 (*p*CO_2), because their calcification produces CO_2 (*36*, *42*). In addition to direct limitation of primary production in the HNLC regions, iron may limit (or co-limit with P) nitrogen fixation by photosynthetic diazotrophs in tropical oceans, where stratification creates high temperature and irradiance and low nitrate concentrations in surface waters, which favor this process (*1*, *43*). The best characterized photosynthetic diazotroph,

Trichodesmium, requires 5 to 10 times more iron for growth based on nitrogen fixation, as compared to ammonium (*47*).

The supply of dust to the oceans is very important in maintaining oceanic primary production and CO_2 uptake but is sensitive to climate change, although the overall effect will vary between ocean biogeochemical provinces (Table 2). In HNLC regions, changes in iron supply will directly affect primary production and species composition, whereas in subtropical/tropical oligotrophic regions, the impact will be mainly via changes in nitrogen fixation. The dust supply from the great North African and Asian deserts directly affects the tropical North Atlantic and temperate North Pacific, respectively, and effects in the two regions can be expected to be different. The largest HNLC region, the Southern Ocean (*36*), has the biggest potential to influence atmospheric CO_2. Here atmospheric dust supply is low (Fig. 2), originating from small dust sources in Argentina, Australia, and South Africa (*6*). Changes in these small and little-studied desert regions may have a disproportionately large global impact.

Because the solubility of iron from dust is low, it follows that there is a large flux of particulate iron through the deep ocean, particularly beneath the major dust plumes. If some of this dust dissolves at depth, it will increase abyssal dissolved iron concentrations and, over the long term, productivity in upwelling regions such as the Southern Ocean. Deep-water dust dissolution will depend on organic ligand concentrations and possibly sediment redox (*33*).

Martin (*49*) proposed that increased dust transport during the last glaciation reduced

iron limitation in HNLC regions, increasing primary production and CO_2 uptake. The complexity of iron biogeochemistry and nutrient co-limitation means that higher glacial dust loadings need not necessarily cause increased productivity. Current models and ice core data yield very different results, predicting that glacial/interglacial changes in dust fluxes will change atmospheric *p*CO_2 by 5 to 45 parts per million (ppm) as a contribution to the total change of 80 to 100 ppm (*19*, *50*). Bopp *et al.* (*50*) reviewed much of the existing marine sediment core data on glacial/interglacial ocean productivity changes and found no simple global pattern of change. However, there are regional patterns (*51*) with increases in productivity in the northwest Pacific, South Atlantic, and Indian Oceans north of the polar front, with decreases south of it. South Pacific productivity appears to be little changed. Some of these patterns can be reproduced in ocean models (*50*).

Effect on Climate of Iron Inputs to the Oceans

The oceans clearly exert a major influence on climate via heat transport and related physical processes (*20*). Large-scale reorganization of oceanic circulation will also affect the transport of iron, effects driven predominantly from within the ocean. Climate change will induce a variety of physicochemical changes in the open ocean, particularly by changing stratification and nutrient supply ratios (*42*), with unpredictable effects. We acknowledge these important issues but focus on the dust cycle, considering now ways in which this can affect the oceans and climate, beside the direct iron limitation of primary production and nitrogen fixation discussed above (Table 2).

Changes in iron fluxes can result in species shifts and changes in phytoplankton size distribution, changing oceanic CO_2 uptake by altering the efficiency of organic carbon export to deep water. Dust may also play a direct role in regulating export via the ballast effect (*52*). In most areas, dust is a minor ballast component compared to opal and calcite, but their production is also influenced by dust/iron supply. Changes in ocean productivity and organic carbon export to deep water will influence subsurface oxygen levels and thereby denitrification in oxygen minima zones, oceanic nitrate inventories and productivity, and nitrous oxide emissions (*53*). Changes in sediment H_2S in such areas could affect deep-ocean iron concentrations and productivity.

Up to eightfold changes in dimethyl sulfide (DMS) concentrations are seen in iron addition experiments (*54*). DMS oxidizes in the atmosphere to form acidic sulfate aerosol, a highly effective scatterer of solar radiation. Modeling suggests that a twofold global rise in DMS fluxes produces a global temperature decrease of 1°C, proving a climate feedback and linking
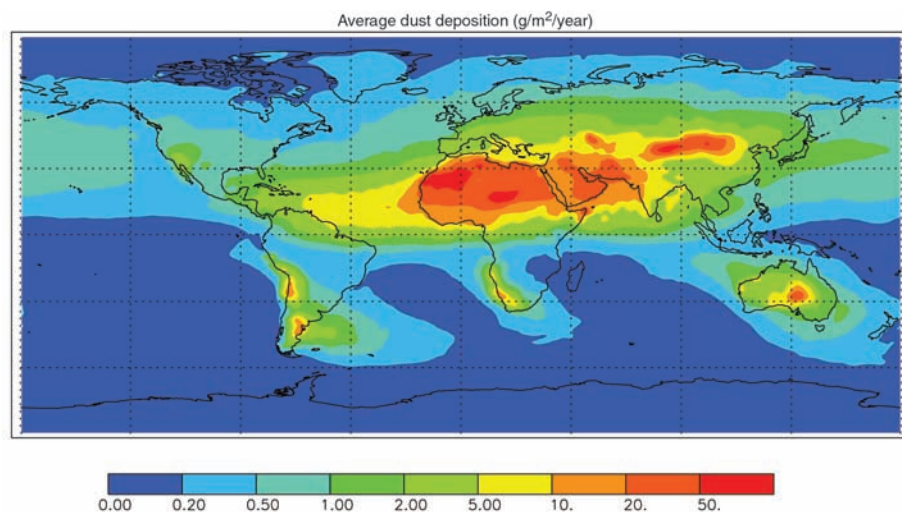

Fig. 2. Dust fluxes to the world oceans based on a composite of three published modeling studies that match satellite optical depth, in situ concentration, and deposition observations (*11*, *14*, *15*). The models have been extensively compared to observations, and although individual models show strengths and weaknesses, this composite appears to match observations well. Total atmospheric dust inputs to the oceans = 450 Tg year^{-1}. Percentage inputs to ocean basins based on this figure are as follows: North Atlantic, 43%; South Atlantic, 4%; North Pacific, 15%; South Pacific, 6%; Indian, 25%; and Southern Ocean, 6%.

the C, Fe, and S cycles (*55*). DMS is only one of a group of trace gases that can influence climate and whose emissions are sensitive to iron concentrations (*54*, *56*, *57*). These include gases that directly affect greenhouse gas forcing (nitrous oxide and methane), ozone cycling (halocarbons and alkylnitrates), and atmospheric oxidizing capacity (isoprene and carbon monoxide). Impacts on ozone are important in radiative forcing (*20*) and via ultraviolet-B impacts on phytoplankton community structure (*42*).

Global Iron Connections

Our analysis demonstrates the complexity of the global iron cycle (Fig. 1). Low iron solubility leads to limitation of marine productivity, with potentially large-scale feedbacks within the global climate system. These could act to either amplify future global climate change via a positive (destabilizing) feedback or diminish it via a negative (stabilizing) feedback. There are considerable uncertainties in our understanding of these interactions, requiring research that integrates across the whole Earth system. We suggest the following research priorities: (i) dust deposition processes, (ii) aerosol iron bioavailability, and (iii) the impact of iron on marine nitrogen fixation and trace gas emissions. These should lead to improvements in global models, allowing realistic predictive capability that can be tested against improved results from the paleo record of the biogeochemical response to changing dust fluxes.

There are discussions about changing terrestrial land uses to create carbon sinks to help mitigate global change. Such changes may reduce dust fluxes to the ocean and thereby reduce primary productivity, offsetting gains in terrestrial carbon storage (*58*). There is also discussion about fertilizing the ocean with iron to increase CO_2 uptake (*59*). Our analysis demonstrates that such a scheme could produce many changes in marine biogeochemical systems. Clearly, we need a comprehensive understanding of the current and future dust/iron cycle before we can contemplate such engineering of the Earth system.

References and Notes

1. P. G. Falkowski, R. T. Barber, V. Smetacek, *Science* **281**, 200 (1998).
2. F. M. M. Morel, N. M. Price, *Science* **300**, 944 (2003).
3. S. M. Kraemer, *Aquat. Sci.* **66**, 3 (2004).
4. S. W. Poulton, R. Raiswell, *Am. J. Sci.* **302**, 774 (2002).
5. R. A. Duce, in *Aerosol Forcing of Climate*, R. J. Charlson, J. Heintzenberger, Eds. (Wiley, Chichester, UK, 1995), pp. 43–72.
6. J. M. Prospero, P. Ginoux, O. Torres, S. E. Nicholson, T. E. Gill, *Rev. Geophys.* **40**, 1002 (2002).
7. T. D. Jickells, L. J. Spokes, in *The Biogeochemistry of Iron in Seawater*, D. R. Turner, K. Hunter, Eds. (Wiley, Chichester, UK, 2001), pp. 85–121.
8. K. S. Johnson, *Global Biogeochem. Cycles* **15**, 61 (2001).
9. N. Brooks, M. Legrand, in *Linking Climate Change to Land Surface Change*, S. McLaren, D. Kniveton, Eds. (Kluwer Academic, Dordrecht, Netherlands, 2000), pp. 1–25.
10. C. S. Zender, D. Newman, O. Torres, *J. Geophys. Res. Atmos.* **108**, 4543 (2003).
11. P. Ginoux et al., *J. Geophys. Res. Atmos.* **106**, 20255 (2001).
12. J. L. Hand et al., *J. Geophys. Res. Atmos.* **109**, D17205 (2004).
13. R. A. Duce et al., *Global Biogeochem. Cycles* **5**, 193 (1991).
14. N. M. Mahowald, C. Luo, *Geophys. Res. Lett.* **30**, 1903 (2003).
15. I. Tegen, M. Werner, S. P. Harrison, K. E. Kohfeld, *Geophys. Res. Lett.* **31**, L05105 (2004).
16. Y. J. Kaufman et al., *J. Geophys. Res. Atmos.* 10.1029/2003JD004436 (2004).
17. Z. S. An, G. Kukla, S. C. Porter, J. L. Xiao, *CATENA* **18**, 125 (1991).
18. D. K. Rea, *Rev. Geophys.* **32**, 159 (1994).
19. R. Röthlisberger et al., *Geophys. Res. Lett.* **31**, L16207 (2004).
20. Intergovernmental Panel on Climate Change, *Climate Change 2001: The Scientific Basis. Contribution of Working Group1 to the Third Assessment Report of the Intergovernmental Panel on Climate Change* (Cambridge Univ. Press, Cambridge, 2001).
21. J. M. Prospero, R. T. Nees, *Nature* **320**, 735 (1986).
22. X. Y. Zhang et al., *Geophys. Res. Lett.* **30**, 10.1029/2003GL018206 (2003).
23. J. M. Prospero, P. J. Lamb, *Science* **302**, 1024 (2003).
24. C. Moulin, I. Chiapello, *Geophys. Res. Lett.* **31**, L02107 (2004).
25. S. D. Schubert, M. J. Suarez, P. J. Pegion, R. D. Koster, J. T. Bacmeister, *Science* **303**, 1855 (2004).
26. C. S. Zhao, X. Dabu, Y. Li, *Geophys. Res. Lett.* **31**, L01103 (2004).
27. M. Claussen, V. Brovkin, A. Ganopolski, C. Kubatzki, V. Petoukhov, *Clim. Change* **57**, 99 (2003).
28. B. J. Huebert et al., *J. Geophys. Res. Atmos.* **108**, 8633 (2003).
29. D. Rosenfeld, Y. Rudich, R. Lahav, *Proc. Natl. Acad. Sci. U.S.A.* **98**, 5975 (2001).
30. D. W. Griffin et al., *Aerobiologia* **19**, 143 (2003).
31. T. D. Jickells, *Mar. Chem.* **68**, 5 (1999).
32. H. J. W. de Baar, J. T. M. de Jong, in *The Biogeochemistry of Iron in Seawater*, D. R. Turner, K. A. Hunter, Eds. (Wiley, Chichester, UK, 2001), pp. 123–253.
33. P. Parekh, M. J. Follows, E. Boyle, *Global Biogeochem. Cycles* **18**, GB1002 (2004).
34. G. Sarthou et al., *Deep-Sea Res. I* **50**, 1339 (2003).
35. V. A. Elrod, W. M. Berelson, K. H. Coale, K. S. Johnson, *Geophys. Res. Lett.* **31**, L12307 (2004).
36. A. J. Watson, in *The Biogeochemistry of Iron in Seawater*, D. R. Turner, K. A. Hunter, Eds. (Wiley, Chichester, UK, 2001), pp. 9–39.
37. K. W. Bruland, E. L. Rue, in *The Biogeochemistry of Iron in Seawater*, D. R. Turner, K. Hunter, Eds. (Wiley, Chichester, UK, 2001), pp. 255–289.
38. M. Gledhill et al., *Mar. Chem.* **88**, 75 (2004).
39. B. Palenik et al., *Nature* **424**, 1037 (2003).
40. G. Rocap et al., *Nature* **424**, 1042 (2003).
41. J. C. Venter et al., *Science* **304**, 66 (2004).
42. P. W. Boyd, S. C. Doney, in *Ocean Biogeochemistry: A Synthesis of the Joint Global Ocean Flux Study (JGOFS)*, M. J. R. Fasham, Ed. (Springer, Berlin, 2003), pp. 157–193.
43. M. M. Mills, C. Ridame, M. Davey, J. La Roche, R. J. Geider, *Nature* **429**, 292 (2004).
44. K. G. Schulz et al., *Nature* **430**, 673 (2004).
45. A. R. Baker, S. D. Kelly, K. F. Biswas, M. Witt, T. D. Jickells, *Geophys. Res. Lett.* **30**, 2296 (2003).
46. T. Oba, T. F. Pedersen, *Paleoceanography* **14**, 34 (1999).
47. A. B. Kustka et al., *Limnol. Oceanogr.* **48**, 1869 (2003).
48. P. W. Boyd et al., *Nature* **428**, 549 (2004).
49. J. H. Martin, *Paleoceanography* **5**, 1 (1990).
50. L. Bopp, K. E. Kohfeld, C. Le Quere, O. Aumont, *Paleoceanography* **18**, 1046 (2003).
51. Z. S. An, J. J. Cao, K. K. Anderson, H. Kawahata, in preparation.
52. R. Francois, S. Honjo, R. Krishfield, S. Manganini, *Global Biogeochem. Cycles* **16**, 1087 (2002).
53. M. A. Altabet, M. J. Higginson, D. W. Murray, *Nature* **415**, 159 (2002).
54. S. M. Turner, M. J. Harvey, C. S. Law, P. D. Nightingale, P. S. Liss, *Geophys. Res. Lett.* **31**, L14307 (2004).
55. G. Zhuang, Z. Yi, R. A. Duce, P. R. Brown, *Nature* **355**, 537 (1992).
56. P. S. Liss, A. Chuck, D. C. E. Bakker, S. Turner, *Tellus,* in press.
57. O. W. Wingenter et al., *Proc. Natl. Acad. Sci. U.S.A.* **101**, 8537 (2004).
58. A. J. Ridgwell, M. A. Maslin, A. J. Watson, *Geophys. Res. Lett.* **29**, 1095 (2002).
59. S. W. Chisholm, P. G. Falkowski, J. J. Cullen, *Science* **296**, 467 (2002).
60. We acknowledge the leadership of the Surface Ocean–Lower Atmosphere Study project (www.solas-int.org) for conceiving this synthesis. We thank the International Council for Science, the United Nations Educational, Scientific and Cultural Organisation, NSF (grants GEO-0402845 and OCE 0228863), the International Geosphere-Biosphere Programme, and the Scientific Committee on Ocean Research for partial support of this work, and B. Sulzberger for her contribution to this work.